Spatial distribution of energy deposited in nitrogen by electrons

John L. Barrett and Paul B. Hays

Space Physics Research Laboratory, Department of Atmospheric and Oceanic Science, The University of Michigan, Ann Arbor, Michigan 48105
(Received 3 July 1975)

The spatial distribution of the energy deposited by kilovolt electrons moving through gaseous molecular nitrogen was measured. The range of electrons of initial energy 300 eV to 5 keV was obtained and can be expressed by the formula $R = K_1 + K_2 E^{A_1} - K_3 E^{A_2}$, where R is the range, E is the initial energy of the electrons, and K_i, A_i are constants. The range, in this energy interval, is greater than that determined by previous measurements. A source of error, not previously discussed, is considered. The energy region (above 1 keV) where the simpler expression $R = KE^A$ holds is discussed. It is shown that this is the energy region where the energy and range dependence of the energy deposition curve can be removed and a normalized, characteristic energy deposition curve λ can be obtained. The efficiency of conversion of electron energy at 1 keV and 280 μ pressure to energy of photons at 3914 Å was measured to be $(0.28 \pm 0.03)\%$.

This work is a study of the spatial distribution of the energy deposited by a beam of electrons injected into gaseous molecular nitrogen. The initial energy of the electron beam was varied from 300 eV to 5 keV. The processes by which electrons lose energy are well known and have been considered by others in the past. However, most previous work has been devoted to energies above 5 keV where, as we shall see, a simple scaling law allows the energy deposition to be universally characterized. This work is concerned with the validity of the scaling law at lower energies.

Previous workers (Grün[1]; Cohn and Caledonia[2]) have used characteristic emissions of nitrogen as a measure of the energy deposited. In the present work the emission of the 0–0 band of the first negative system of N_2^+ at 3914 Å will be used. It has been shown (Rapp and Englander-Golden[3]; McConkey, Woolsey, and Burns[4]; Borst and Zipf[5]) that 0.07 photons of 3914 Å wavelength are produced for each ionization of N_2 independent of the energy of the exciting electron for energies from 30 eV to 3 keV. This fraction is the ratio of the cross section for excitation to the $B\,^2\Sigma_u^+$ 0–0 band state to the total ionization cross section for N_2. Furthermore, the total number of ionizations produced by an electron is approximately proportional to its initial energy. Therefore, the number of photons of 3914 Å radiation emitted from a volume of the gas is approximately proportional to the energy deposited in that volume independent of electron energy. This proportionality is illustrated in Fig. 1 which is a plot of the energy loss per unit path length, $1/n\ dE/dX$, and of the cross section for excitation to the $B\,^2\Sigma_u^+$ state (Green and Stolarski[6]), as a function of electron energy.

I. PREVIOUS WORK

Grün[1] measured the total luminosity of 3914 Å radiation in N_2 in planes perpendicular to the axis of the electron beam which had an initial energy of 5 to 54 keV. He was able to express the range of the electrons (in g/cm^2) by

$$R = CE_0^A\ , \tag{1}$$

where E_0 is the initial energy of the beam in kilovolts, $A = 1.75$, and $C = 4.57 \times 10^{-6}$ g/cm^2. The units of range commonly used in the literature, g/cm^2, is the product of the density, g/cm^3, times the distance in cm. For a 5 keV beam he measured the range to be 7.65×10^{-5} g/cm^2 which, at 10^{13} cm^{-3} (about 100 km), equals a distance of 1.57 km.

Taking the energy deposition curves, α, and factoring the initial energy and range according to

$$\alpha = (E_0/R)\lambda(Z)$$
$$Z = X/R \tag{2}$$

a dimensionless distribution function λ was obtained by Grün. α has the dimensions eV/g/cm^2 and is the energy deposited in a slab of unit thickness, X is the distance along the beam in g/cm^2, and Z is the fraction of the range travelled. His curves of λ from 5 to 54 keV have the same shape and lie nearly upon each other.

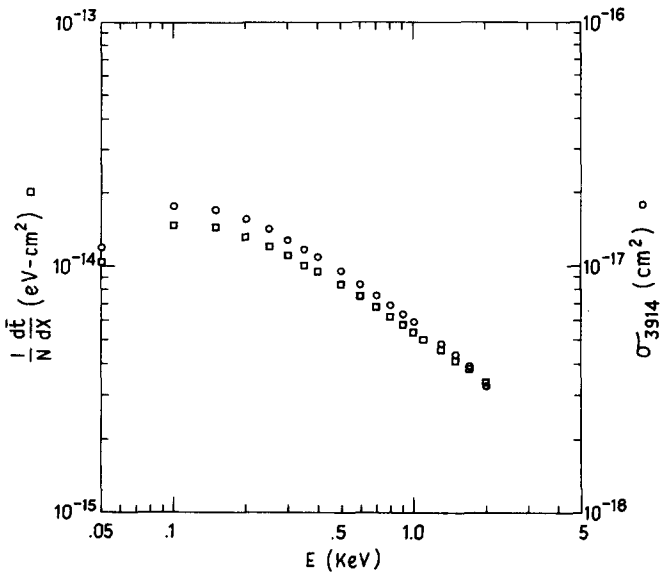

FIG. 1. Comparison of energy loss (□) with σ_{3914}(○), calculated from Green and Stolarski,[6] as a function of energy. The two curves have the same shape over this energy interval.

Rees[7] used Grün's expression for the range down to 5 keV in a work on the penetration of electrons into the earth's atmosphere. For energies from 5 keV to 300 eV Rees fitted a curve to values of the range calculated by Maeda,[8] derived from experimental energy loss data, from Dalgarno,[9] who calculated the stopping power from the relativistic Bethe formula, and from measurements of Alper[10] who used a cloud chamber to determine the path length of secondary electrons released by α particles from nuclear decays. The range taken from Rees' curve agrees with the range measured in this work down to 1 keV, but are increasingly short below that. At 300 eV the range is 26 percent shorter than that measured here.

Cohn and Caledonia[2] measured the intensity profiles of 3914 Å with electron beams of from 2 to 5 keV initial energy. They found that the range at those energies can be expressed by Eq. (1) with the same constants Grün determined to within the accuracy of their measurements. They also plotted a normalized distribution function and compared it with Grün's data and found agreement.

Hartman[11] measured the efficiency of conversion of electron energy into energy of 3914 Å photons as a function of initial electron energy from 165 eV to 1 keV. He found the efficiency as a function of pressure from 30 to 960 μ. The efficiency was independent of pressure below 100 μ, but decreased with increasing pressure above 100 μ. In the pressure-independent region he determined the efficiency to be 0.34 percent. His pressure-corrected value is in agreement with the efficiency determined here.

In the present work Grün's scaling relation [Eq. (2)] is used on the data taken to generate the dimensionless curves, λ. The low energy limit where the curves, λ, are no longer identical is determined. It will be shown in Sec. II that the range energy relation [Eq. (1)] is a limiting case of a more general expression.

The longitudinal distribution of energy deposited has been calculated by Lewis[12] and Spencer.[13] They treated the spreading of the electron beam as a diffusion problem and solved the diffusion equation numerically.

A different approach was taken by Berger, Seltzer, and Maeda[14] who performed a Monte Carlo calculation using Bethe's formula (Rohrlich and Carlson[15]) for continuous energy loss down to 200 eV with a shielded Coulomb scattering potential to obtain the spatial distribution of energy. They were able to reproduce the spatial distributions of Grün and of Cohn and Caledonia. In a later work Berger *et al.*[16] discussed the energy degradation of initially monoenergetic electrons. They obtained the transverse as well as the longitudinal distribution of energy deposited in the gas, together with the energy distribution of the electrons along the beam. The calculations do not give a simple expression either for the range of the electrons as a function of their initial energy or for the energy of electrons along their path.

II. CALCULATIONS

A. Range and energy of electrons in nitrogen

This section presents a simplified method of calculating the range of electrons in a gas and shows that an expression of the form obtained by Grün [Eq. (1)] can be obtained in the limit of higher energies (greater than 1 keV).

The energy loss rate in an interval can be written

$$dE/dX = nL(E) \equiv n\Sigma\sigma_j \delta E_j \,, \tag{3}$$

where σ_j is the cross section, δE_j is the energy lost in exciting the jth state, and $L(E)$ is the loss function.

If the cross sections and energy differences are known, Eq. (3) can be used to solve for the range

$$R(E_0) = \int_0^{E_0} \frac{dE}{dE/dX} = \frac{1}{n}\int_0^{E_0} \frac{dE}{L(E)} \,. \tag{4}$$

Green and Stolarski[6] give analytic representation of the cross sections required by Eq. (3). In the present work the reciprocal of the loss function was evaluated using these representations and the results plotted. The resulting curve was represented to within 1 percent down to 30 eV by a sum of two terms, $1/L = 8.49 \times 10^{-11}E^{1.67} + 33.7\times 10^{-7}E^{-1.7}$, where E is in eV, and L is in eV cm^2. As the range of 30 eV electrons is negligible this fit was used in Eq. (4), resulting in

$$R = 4.30\times 10^{-7} + 5.08\times 10^{-11}E_0^{1.67} - 48.1\times 10^{-7}E_0^{-0.7} \,, \tag{5}$$

with E_0 expressed in eV and R in g/cm^2. For energies above 1 keV the second term dominates the expression, giving the range in the form of Eq. (1).

The Born–Bethe approximation (Rohrlich and Carlson[15]) for the rate of energy loss has dE/dX proportional to $(\log E)/E$. Our expression comes from the use of the approximation of $\log E$ by $E^{1/3}$ to $E^{1/4}$ so $(\log E)/E$ is $E^{-2/3}$ to $E^{-3/4}$. The approximation holds for the argument ranging about an order of magnitude. When E is expressed in keV, E/E_0 is dimensionless. Using the approximation for $\log E$ one obtains

$$R \sim \int_0^{E_0} \frac{dE}{\log E/E} \sim E^{1.66} \text{ to } E^{1.75} \,.$$

This range measured in this work agrees closely with the value calculated in Eq. (5).

III. APPARATUS

The apparatus, shown schematically in Fig. 2, consists of a vacuum system which is divided into an interaction region and a differentially pumped region, an electron gun and the optics. Electrons are injected into an interaction region that is filled with nitrogen at high (50–5000 μ) pressure. The electrons lose their energy by exciting and ionizing the gas, which results in various optical emissions. A photometer, looking into the interaction region (shown dotted in the figure) will count the number of photons of a particular wavelength along the line of sight.

The $A\Omega$ (A is the area of the collecting lens, Ω is the solid angle subtended by the field stop at the collecting

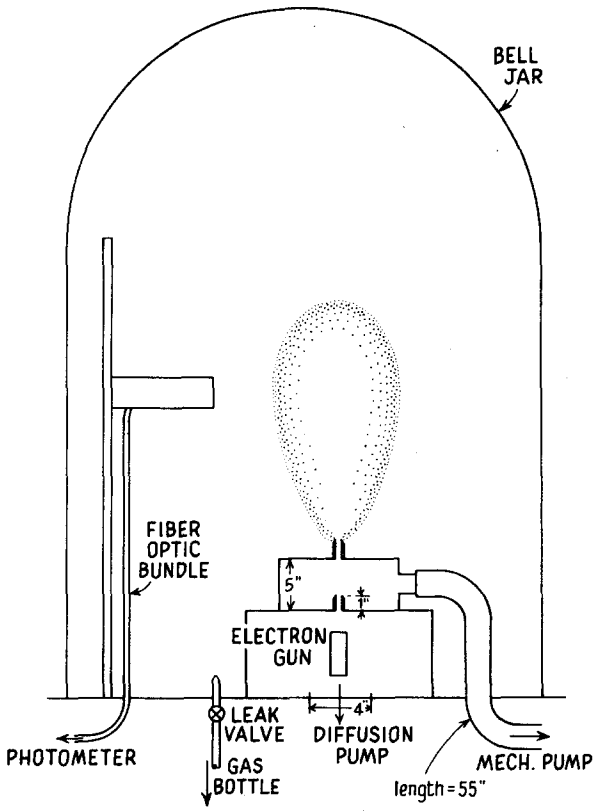

FIG. 2. Apparatus. The dotted area shows the general shape of the interaction region.

lens) of the system is defined by a lens (8 mm diam, 81 mm focal length) and an aperture (2.2 mm diam), 17.8 cm behind it. A Ω has a value of 5.95×10^{-5} cm^2 sr. Directly behind the aperture is an 83 cm length of fiber optic bundle which leads the light from the vacuum system to a photometer.

The entire system, input optics to scaler–timer, was calibrated against a National Bureau of Standards secondary standard to convert the counting rate to a surface brightness using the method discussed in Sharp.[17]

IV. RESULTS

A. Radial distribution

The surface brightness as a function of radial distance from the beam axis is shown for 300 eV at a number of axial distances, ρ, in Fig. 3. ρ, like Z, is expressed as a fraction of the range and is dimensionless. In order to obtain the volume emission rates it is necessary to perform an Abel inversion of the data. The data were fitted piecewise to overlapping quadratics according to the scheme in Roble and Hays.[18] Figure 4 shows the radial distribution at 5 keV measured at $Z=0.5$ compared with the results of a calculation by Berger.[16] The two curves agree well out to $\rho=0.7$ where they both go to zero. Figure 5 shows the radial distribution at $Z=0.7$. The two curves have the same shape out to $\rho=0.4$ at which point the calculated value falls faster than the measured value. At this value of Z the luminosity calculated is slightly below the measured value. Agreement with Berger's calculation might be improved if he followed the secondaries of lower initial energy.

In summary, the radial distribution of energy deposition along the beam axis has been measured and shows good agreement with Monte Carlo calculations, but indicates that the theories need further work near the end of the range.

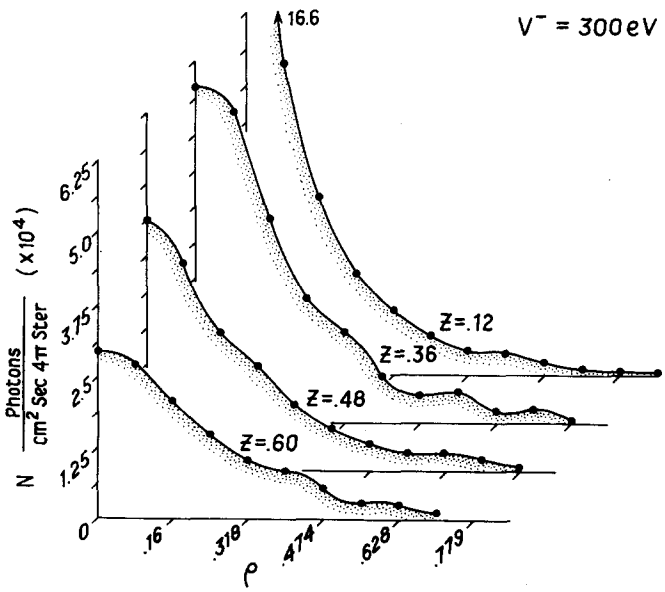

FIG. 3. Radial distribution of energy deposited by a beam of 300 eV electrons.

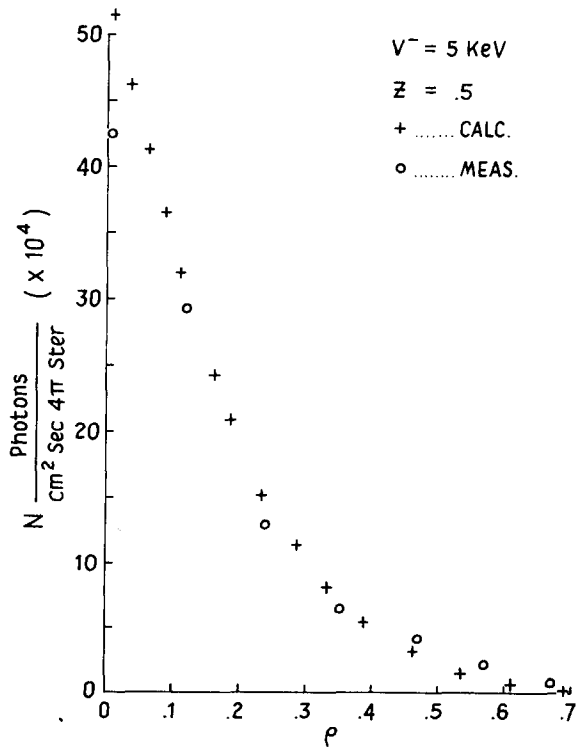

FIG. 4. Measured and calculated radial distributions; $Z=0.5$. Straggling of secondary electron of initial energy down to 200 eV is considered in the calculation.

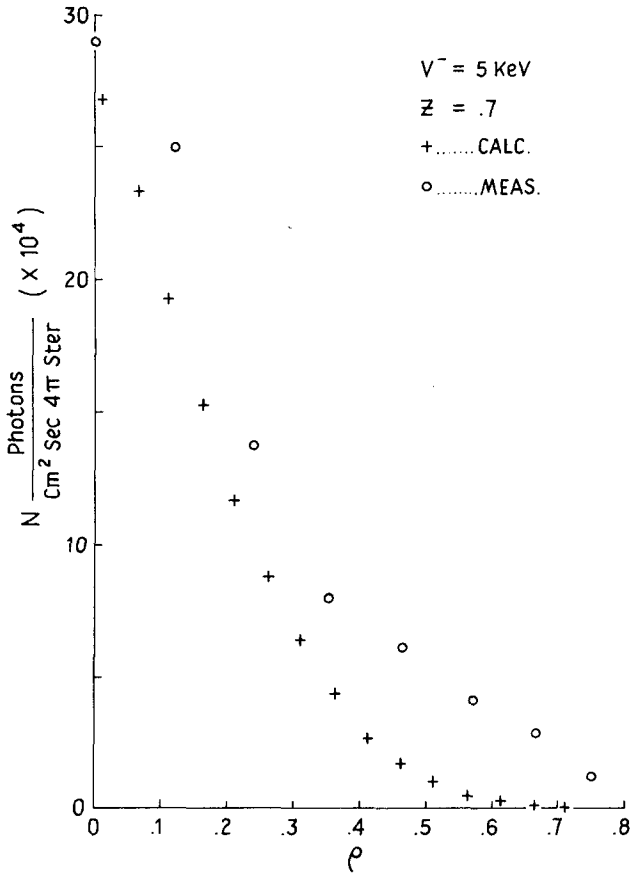

FIG. 5. Measured and calculated radial distributions; $Z = 0.7$.

B. Range

For each run at each energy, the energy deposited in each plane was plotted on the vertical axis with the position of the plane on the horizontal axis. In every case the end of the curve has a linear portion followed by a curved tail. The tail is a reflection of energy straggling. Once the beam starts interacting with the gas it is no longer monoenergetic. The various electrons will penetrate to different depths. However, the linear portion of the curve may be extrapolated to the axis, as in Fig. 6 to define a mean range for the beam. Runs taken at the same initial energy were not always at the same pressure. The various distances were expressed in mass path,

$$g/cm^{-2}\ (X\ cm \times n\ g/cm^{-3})$$

so that the pressure need not be an explicit factor. Fig-

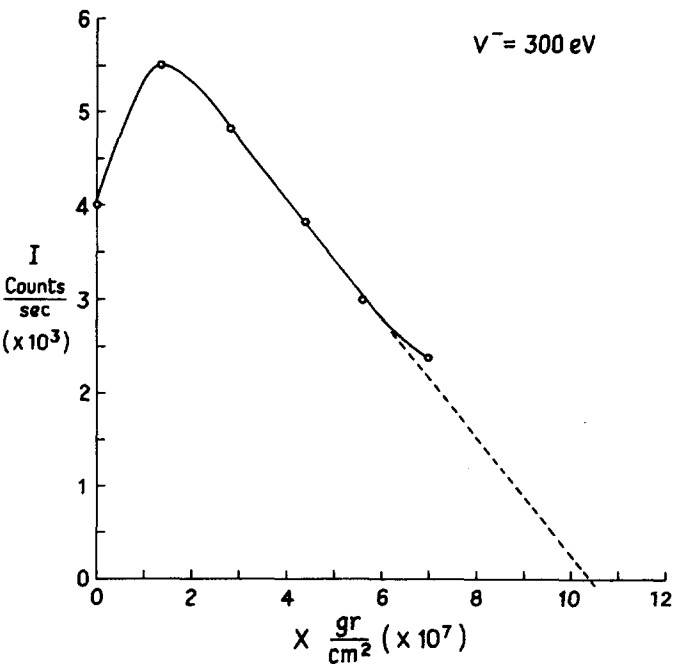

FIG. 6. Range for 300 eV.

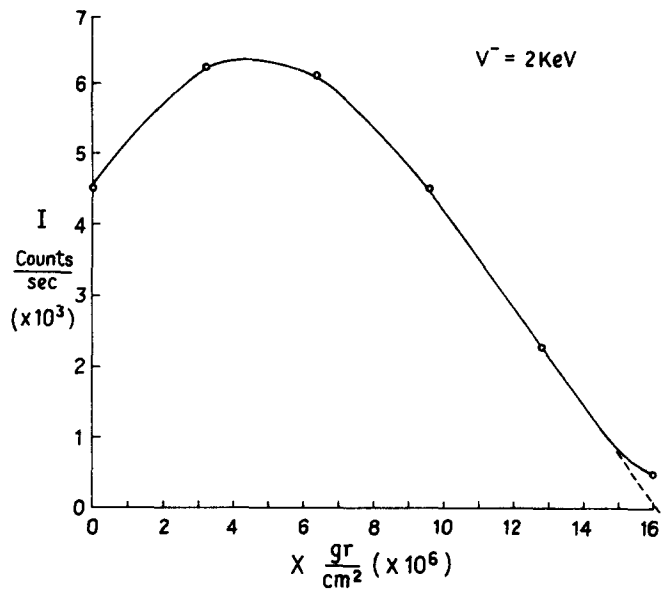

FIG. 7. Range for 2 keV.

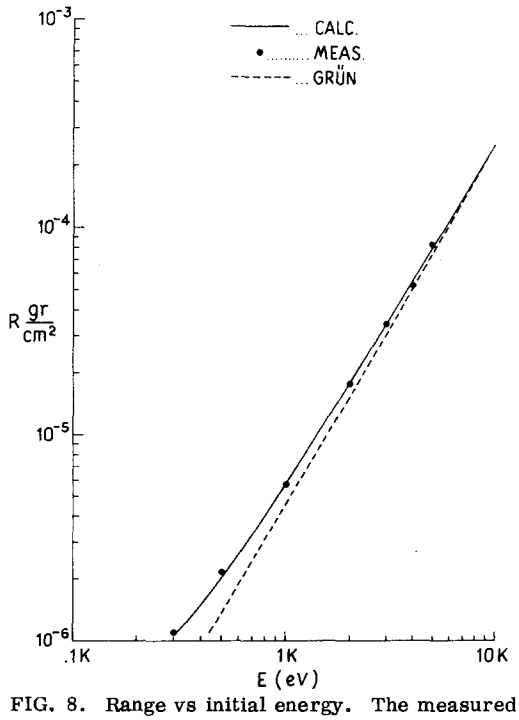

FIG. 8. Range vs initial energy. The measured values of range lie very close on the curve calculated from Eq. (5). The dashed curve is an extrapolation of Grüns expression for the range to energies below 5 keV.

ure 6 is the range curve for 300 eV, Fig. 7 is the range curve for 2 keV.

The mean range for each initial energy was calculated and a plot was made, Fig. 8 of the $\ln R$ versus E_0. It can be seen from the figure that the points down to 1 keV lie closely on a line of slope 1.66. This line gives a relation between range and energy, for those points lying on the line, of

$$R = KE^{1.66} \tag{6}$$

with $K = 5.5\times10^{-6}$ g/cm^2. The line curves upward for energies below 1 keV in accordance with the calculation discussed in Sec. II using all the terms of Eq. (5). The measured range at 300 eV and at 500 eV is seen to be in agreement with this curve. For purposes of comparison the expression for the range determined by Grün is extrapolated into this region. It can be seen that it increasingly underestimates the range of electrons at lower energies. In Sec. II the expression for the range

$$R = CE_0^A$$

was discussed. This would be a straight line on the plot (Fig. 8). The values of the range measured for initial energies below 1 keV are greater than those predicted by Eq. (1). The more exact expression [Eq. (5)] is also plotted and is in close agreement with the measured values.

As discussed in Sec. II, it is the use of the Born approximation in the high energy limit which puts the range in the form of Eq. (1). As the fraction of the electron's energy below 200 eV (the approximate energy where the high energy limit no longer agrees with the measured cross section) becomes an increasing part of its total energy the range will depart from Eq. (1) and the shape of the energy loss curve will change. The actual cross section in N_2 rises more slowly than the high energy limit of the Born approximation from 200 to 100 eV, then begins to drop. Since the loss function L is proportional to the cross section and therefore the range is inversely proportional to the cross section, the range will be greater at low energies than that predicted by Eq. (1). Scattering of the electrons will decrease the depth of penetration into the medium, but not their range. The definition of range is such that only electrons with no appreciable deflection contribute to the determination of the range. The measured ranges are listed in Table I together with the ranges calculated from the loss function.

The cross sections used in the calculations are known to within 10 percent. Since all allowed transitions have the same functional dependence on energy (where the Born approximation holds) the slope of the $\ln E$ vs $\ln R$ curve will not change if the cross sections are systematically incorrect. If all the cross sections were systematically high or low the y intercept of the curve would be changed. This would affect the constant C in Eq. (1) and make all the ranges be systematically low or high. Since the data are not displaced from the calculated curve the cross sections are not systematically incorrect.

It is important to know the energy of the electron beam as it leaves the nozzle and enters the interaction region. The accuracy to which it is known will determine the accuracy of the range. The accelerating voltage of the electrons at the vacuum flange is measured to better than 0.1 percent. The major concern is whether they lose energy before reaching the interaction region.

TABLE I. Range.

E_0(keV)	R_{fit}	R_{meas}	R_{calc}
0.3	7.47×10^{-7}	1.06×10^{-6}	1.055×10^{-6}
0.5	1.74×10^{-6}	2.16×10^{-6}	2.05×10^{-6}
1.0	5.50×10^{-6}	5.72×10^{-6}	5.757×10^{-6}
2.0	1.74×10^{-5}	1.77×10^{-5}	1.754×10^{-5}
3.0	3.41×10^{-5}	3.43×10^{-5}	3.418×10^{-5}
4.0	5.50×10^{-5}	5.23×10^{-5}	5.509×10^{-5}
5.0	7.97×10^{-5}	8.30×10^{-5}	7.985×10^{-5}

$R_{fit} = 5.50\times10^{-6}E_0^{1.66}$ E_0 in keV
All R in g/cm^2

From the filament to the final nozzle the mass path of the electrons is less than 0.1 percent of the range. This is simply determined from the pressure along the path and the path length. The situation at the final nozzle is not so easily interpreted. For the operating pressure and the nozzle diameters chosen, the gas flow through the nozzle is midway between viscous and molecular flow. The mass distribution has not been calculated for such a case, however, limits are estimated below.

The distributions of pressure for the viscous flow and molecular flow regions have been calculated (Barrett[19]). In viscous flow the pressure drops very slowly until right at the exit where it goes steeply to the lower pressure. The average pressure in the nozzle is 67 percent of the pressure in the interaction region. In molecular flow the pressure dependence is different. The pressure drops linearly from the nozzle. The latter case requires 50 percent of the nozzle length correction to the range while the former, viscous flow, requires a 67 percent correction.

In each case it was determined what fraction of the distance the system was from the molecular flow to the viscous flow region. The corresponding fraction of distance between 0.5 and 0.67 was used as the fraction of the input pressure chosen as the average pressure in the nozzle and the corrections to the range was evaluated accordingly. The corrections ranged from 2 to 8 percent.

Cohn and Caledonia do not discuss a correction to the range due to the passage of the electrons through the nozzle. Grün mentions as negligible (less than 0.6 percent) corrections to the range from the chamber before the last nozzle. He does not discuss the last nozzle. The diagram of Grün's apparatus shows a much smaller path through his nozzle which may make the mass path through it negligible.

Figure 8 shows the measured values of range (corrected for nozzle) plotted as a function of initial energy.

The only point measured in common with Grün is at 5 keV. At that point the range measured here was higher than his by 7.8 percent. Cohn and Caledonia get a range at 2 keV equal to 1.54×10^{-6} g/cm^2 which is lower than the value measured here by 12 percent. This may be due to the neglect of the energy loss of the beam in the nozzle by Cohn and Caledonia as discussed above.

In summary the range in N_2 has been measured from 300 eV to 5 keV and is in agreement with calculated values. It can be expressed, over this range of energy, by

$$R = 4.30\times10^{-7} + 5.36\times10^{-6}\times E_0^{1.67} - 0.38\times10^{-8}E_0^{7} .$$

C. Energy of the electrons along their path

Equation (1) can be used to obtain the mean energy of the electrons, $E(X)$, at some point X along their path. Assume the electrons have travelled a distance X and have mean energy $E(X)$ at that point. That energy is just sufficient for them to travel $R-X$. Electrons starting from X have a range $R-X$ and an energy $E(X)$,

$$R - X = CE(X)^A . \tag{7}$$

Dividing Eq. (7) by Eq. (1) we obtain

$$E = E_0(1 - X/R)^{1/A} . \tag{8}$$

Since the range energy Eq. (1) only holds down to 1 keV Eq. (8) might be expected to give inaccurate results if the initial energy is sufficiently low. An initial energy of 1 keV is used and the energy of the beam is compared with that obtained by a more accurate method [discussed below, Eq. (10)] in Fig. 9. It can be seen that even in this extreme case Eq. (8) gives good agreement out to $Z = 0.9$.

Stolarski[18] integrated the universal energy loss curve out to X/R to obtain the mean energy

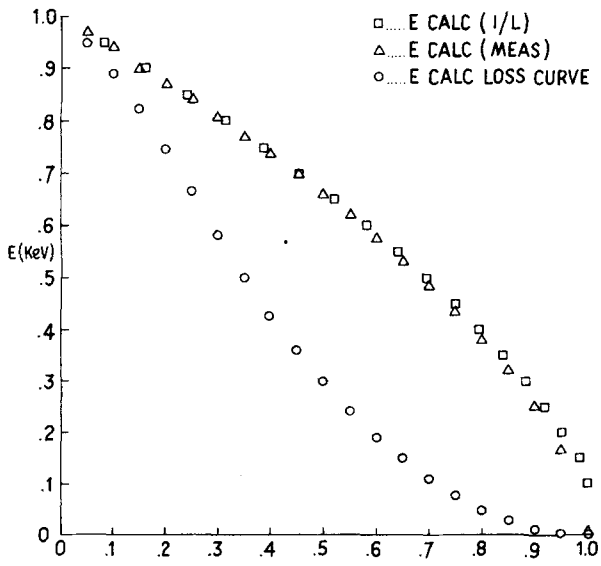

FIG. 9. Energy of beam (initial energy of 1 keV) along the Z axis obtained from Eqs. (9) (○), (6) (△), (5) (□). The simpler Eq. (6), gives very good agreement with the more exact result out to $Z = 0.9$.

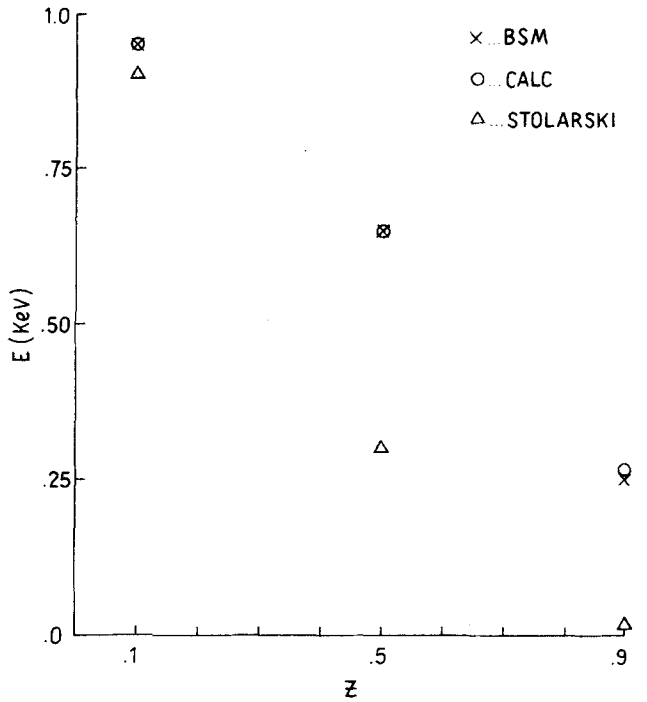

FIG. 10. Comparison of the energy of the electrons along their path calculated in this work (calc) with the mean energy from a Monte Carlo calculation (BSM). The two methods give very close agreement. The results of Eq. (9) are shown here to have a different shape.

$$E = E_0\left(1 - \int_0^{X/R} \lambda\, d\frac{X}{R}\right) . \tag{9}$$

Equations (8) and (9) give different shapes for the energy of the beam along the axis. Equation (4) can be modified so that the energy loss in traveling a distance X can be computed

$$X = \int_{E_0}^{E} \frac{dE}{dE/dX} . \tag{10}$$

The three curves so obtained are plotted in Fig. 9. It is seen that the energies calculated by Stolarski's method are low in the middle of the curve compared to the other two calculations which agree. Stolarski assumed that the energy deposited in a plane was the energy lost by the beam to that point. In fact some fraction of the energy deposited in a plane comes from electrons which suffered appreciable deflections and are, therefore, at a lower energy in that plane, which lowers the average energy of the electrons at that Z. Berger, Seltzer, and Maeda[16] calculate the flux of electrons along the axis of the beam. They show the flux at 10 percent, 50 percent, and 90 percent of the range. The mean value of the energy at each of these points is plotted in Fig. 10 together with the calculations from Eqs. (8) and (9).

D. Axial distribution

Figure 11 shows, λ, the normalized fractional energy deposition distribution of Eq. (2), taken from 1, 2, and 3 keV with the energy and range dependence factored out. It is seen that they fit closely upon one another. In Fig. 12 the curves for 300 and 500 eV are contrasted with that for 1 keV. While the peaks of the 1 keV and

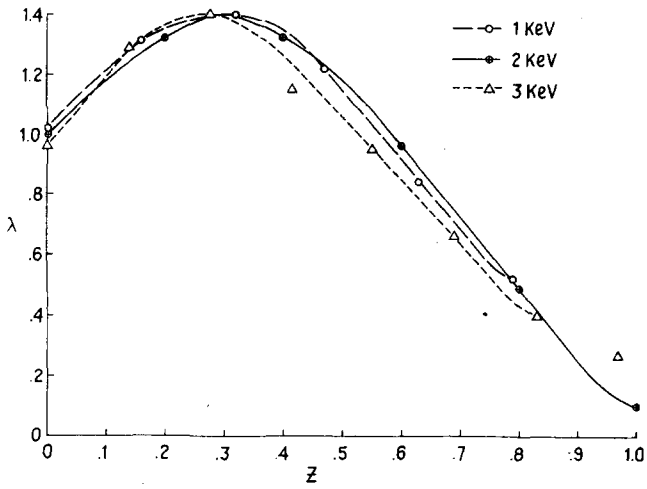

FIG. 11. Normalized curves of energy deposition. λ is obtained from the data using Eq. (2). Z is the fraction of the range.

higher energies occur at $Z = 0.3$, the peaks at the lower energies are moving to lower values of Z and the curves no longer have the same shape. This corresponds to the deviation of the measured range from the relation given by Eq. (1) for energies below 1 keV.

E. Efficiency of conversion of electron energy to 3914 Å

The energy deposition curves can be used to determine the number of photons emitted in planes between those measured. Integrating the area under the curve gives the total number of counts that would be obtained if space were completely scanned. The geometry and transmission of the optics are known from calibration.

These can be used to determine the total number of photons emitted in the interaction region of the gas. Multiplication by $h\nu$ gives the total energy of 3914 Å photons per second.

Since the voltage at which the electrons are injected is known and the current is monitored, the power input is known. Dividing this into the energy of 3914 Å photons gives an efficiency of conversion at the pressure at which the measurement is made. Using the data for 1 keV an efficiency of (0.28 ± 0.03) percent is calculated.

Hartman[11] measured an efficiency of conversion of electron energy to photon energy at 3914 Å of 0.34 percent at low (below 100 μ) pressure. He measured the efficiency at a number of higher pressures up to 960 μ. His results were used to obtain the efficiency at 280 μ, the pressure where efficiency was determined in this work. The value of 0.34 percent is multiplied by 0.72, the pressure correction, to obtain a value of 0.25 percent. This compares reasonably well with the value determined here of 0.28 ± 0.03 percent.

In order to determine what effect O_2 has on the efficiency he measured a mixture of N_2 and O_2. At a total pressure of 60 μ partial pressure of oxygen, there is no effective quenching due to O_2. At a total pressure of 60 μ, O_2 was made an increasing fraction of the pressure. The total amount of 3914 Å radiation was directly proportional to the fraction of N_2 in the mixture, indicating that, up to 60 μ partial pressure of oxygen, there is no effective quenching due to O_2.

Brocklehurst and Downing[20] give the gas kinetic reaction coefficient for quenching the $B\,^2\Sigma_u^+$ state as 2.5×10^{-10} cm^3/sec. The Einstein coefficient for transition to the ground state of the ion is (Banks and Kockarts[21]) 1.07×10^7 sec^{-1}. The Stern–Vollmer factor, which gives the loss of radiation due to quenching, is

$$\text{S.V.} = \frac{1}{1 + Kn[N_2]/A} = 0.81 ,$$

where $n[N_2] = 10^{16}$. This is reasonable agreement with the value Hartman determines which is 0.72, inasmuch as the quenching coefficient K is only accurate to 36 percent.

V. CONCLUSIONS

The radial and axial distributions of energy deposited in gaseous molecular nitrogen by electron beams of initial energy from 300 eV to 5 keV have been measured. The axial distribution measured in this work, expressed as a characteristic, dimensionless curve agrees with that measured by Grün for initial electron energies above 1 keV. Below that energy the shape of the curve changes with energy. The form of the range relation and the shape of the loss curve is seen to be a high energy limiting case of the range relation and loss curve determined in this work. The radial distributions measured here agree with distributions calculated by Berger *et al.*[16] except at large radial and axial distances.

The range of electrons was determined from the axial distributions. The values were found to be in agreement with the relation

$$R = 4.30 \times 10^{-7} + 5.36 \times 10^{-6} E_0^{1.67} - 0.38 \times 10^{-8} E_0^{0.7}$$

which is obtained from the stopping power. For energies from 1 to 5 keV the data can be fit to the expression

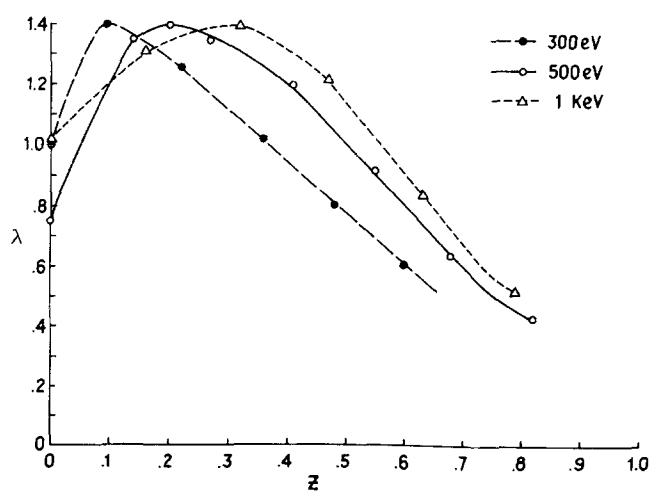

FIG. 12. λ is the normalized energy deposition distribution. The curves for initial energies below 1 keV do not have the same shape as the 1 keV curve. Contrast this with Fig. 11 where it is seen that the curves obtained from higher energies have the same shape.

$$R = 5.50\times10^{-6}E_0^{1.66}$$

which is in the same form as the expression obtained by Grün for energies from 5 to 54 keV.

In the range where this equation is valid the energy of the beam, at a point X along the beam axis can be determined from

$$E = E_0(1 - X/R)^{0.6} .$$

The more exact expression, Eq. (4), can be used to obtain the energy by replacing the lower limit of the integral with an energy E

$$X = \int_E^{E_0} \frac{dE}{dE/dX} ,$$

where X is the point at which the mean energy is E.

The conversion efficiency of electron energy at 1 keV and a pressure of 280 μ of nitrogen to 3914 Å radiation is measured to be (0.28 ± 0.03) percent in agreement with a similar measurement by Hartman.

ACKNOWLEDGMENTS

The authors are grateful to Dr. Richard S. Stolarski and Professor Jens C. Zorn for discussions of this work. Financial support received from National Aeronautics and Space Administration Grant NGR 23-005-360 and from NSF Grant GA-38290 is gratefully acknowledged.

[1]A. E. Grün, Z. Naturforsch. A 12, 89 (1957).
[2]A. Cohn and G. Caledonia, J. Appl. Phys. 41, 3767 (1970).
[3]D. Rapp and P. Englander-Golden, J. Chem. Phys. 43, 1464 (1965).
[4]J. W. McConkey, J. M. Woolsey, and P. J. Burns, Planet. Space Sci. 15, 1332 (1967).
[5]W. L. Borst and E. C. Zipf, SRCC Report #108, University of Pittsburgh, 1969.
[6]A. E. S. Green and R. S. Stolarski, J. Atmos. Terr. Phys. 34, 1703 (1972).
[7]M. H. Rees, Planet. Space Sci. 12, 722 (1964).
[8]K. Maeda, J. Geophys. Res. 68, 185 (1963).
[9]A. Dalgarno, Ann. Geophys. 17, 16 (1961).
[10]T. Alper, Z. Phys. (Leipz.) 76, 172 (1932).
[11]P. L. Hartman, Planet. Space Sci. 16, 1315 (1968).
[12]H. W. Lewis, Phys. Rev. 78, 526 (1950).
[13]L. V. Spencer, Phys. Rev. 98, 1597 (1955).
[14]M. J. Berger, S. M. Seltzer, and K. Maeda, J. Atmos. Terr. Phys. 32, 1015 (1970).
[15]F. Rohrlich and B. C. Carlson, Phys. Rev. 93, 38 (1954).
[16]M. J. Berger, S. M. Seltzer, and K. Maeda, J. Atmos. Terr. Phys. 36, 591 (1974).
[17]W. E. Sharp, Ph.D. thesis, University of Colorado, 1970.
[18]R. S. Stolarski, Planet. Space Sci. 16, 1265 (1968).
[19]J. L. Barrett, Ph.D. thesis, University of Michigan, 1975.
[20]B. Brocklehurst and F. A. Downing, J. Chem. Phys. 46, 2976 (1967).
[21]P. M. Banks and G. Kockarts, *Aeronomy* (Academic, New York, 1973), Part A.